Titel/Title: **Limited influence of climate change mitigation on short-term glacier mass loss**

Autor*innen/Author(s): Ben Marzeion, Georg Kaser, Fabien Maussion, & Nicolas Champollion

Limited influence of climate change mitigation on short-term glacier mass loss

Ben Marzeion[1], Georg Kaser[2], Fabien Maussion[2], & Nicolas Champollion[1]

January 26, 2018

[1]Institute of Geography, University of Bremen, Germany
[2]Department of Atmospheric and Cryospheric Sciences, Universität Innsbruck, Austria

Glacier mass loss is a key contributor to sea-level change[1, 2], to slope instability in high-mountain regions[3, 4], and to the changing seasonality and volume of river flow[5, 6, 7]. Understanding the causes, mechanisms, and time scales of glacier change is therefore paramount to identifying successful strategies for mitigation and adaptation. Here, we use temperature and precipitation fields from CMIP5 output to force a glacier evolution model, quantifying mass responses to future climatic change. We find that contemporary glacier mass is in disequilibrium with the current climate, and that 36 $\pm$ 8 % mass loss is already committed in response to past greenhouse gas emissions. Consequently, mitigating future emissions has only a very limited influence on glacier mass change in the 21st century. No significant differences between 1.5 K and 2 K warming scenarios are detectable in the sea-level contribution of glaciers accumulated within the 21st century. In the long-term, however, mitigation will exert a strong control, suggesting ambitious measures are necessary for the long-term preservation of glaciers.

On time scales of many millenia and longer, glaciers are shaped through interaction with their bedrock[8, 9, 10]. On millennial and shorter time scales, their geometry is an expression of the atmospheric conditions surrounding them[11, 12]: Positive (negative) mass balances lead to an expansion (retreat) of the glacier to lower (higher) terminus elevations. This mechanism provides a negative feedback[13] through which glaciers adjust their elevation-area distribution to the atmospheric forcing. However, the signal of a perturbed mass balance is distributed over the glacier at a finite velocity, which results in a lagged response of the glacier length to changes in mass balance forcing[14, 15]. During periods when climate change happening rapidly relative to the glaciers' response times, glaciers may therefore experience a strong disequilibrium with climate conditions[16]. The amount of ice stored in glaciers[39, 18] at any given time may therefore contain a substantial fraction that is not sustainable under concurrent climate conditions.

To quantify this disequilibrium, we first estimate the glacier mass that is sustainable under different global mean temperatures. Note that the spatial distribution of glaciers relative to the spatial pattern of atmospheric temperature change implies that glaciers on average experience higher atmospheric temperature changes than the global mean [13]. We consider all glaciers globally, but exclude peripheral glaciers in Greenland and Antarctica as well as the ice sheets. Using anomaly fields of temperature and precipitation obtained from the Coupled Model Intercomparison Phase 5 (CMIP5) model ensemble and gridded climate observations from the period 1961 to 1990[19, 20], we force a global glacier evolution model to quantify the long-term response of each glacier contained in the Randolph Glacier Inventory (RGI) version 5[21], which provides initial surface area and elevation distribution values, to these anomaly fields. This was achieved by repeatedly applying identical climate forcing, corresponding to a given global mean temperature change, to each glacier, until the volume change of the glacier became negligible (see Methods for details of the setup of the experiment). The results, shown in Fig. 1, indicate a strong disequilibrium between the present-day global glacier mass and present-day climate conditions (when referring to present-day glacier mass, we refer to the year 2015; for present-day climate conditions we refer to the mean over the years 2006 to 2015), consistent with current in-situ observations of glacier mass change[22]. While our estimate of present-day glacier mass is 307 $\pm$ 18 mm sea-level equivalent (mm SLE, the uncertainty indicates the 90 % confidence interval), the sustainable ice mass is estimated to 195 (173 to 222) mm SLE (the numbers in brackets indicate the 5th and 95th percentiles of the glacier model ensemble), indicating that 36 (28 to 44) % of the present-day ice mass are unsustainable and would melt, if the current climate remained stable for the coming centuries. This number is close to previous estimates of 27 $\pm$ 5 %[23] (for the reference year 2006) and 38 $\pm$ 16 % [24] (for the reference period 2000 to 2010) of already committed, but not yet realized glacier mass loss, obtained from observed accumulation area ratios. To sustain present-day ice mass, the global mean temperature would have to drop to pre-industrial conditions (when referring to pre-industrial, we refer to the mean over the years 1850 to 1879). This finding is consistent with previous results that indicate glaciers where strongly responding to the end of the preceding, cooler period of the Little Ice Age, before anthropogenic warming became the dominant cause of their mass loss in the second half of the twentieth century[25]. Further global warming increases the present day commitment to future ice mass loss to 159 (115 to 179) mm SLE and 191 (139 to 205) mm SLE for 1.5 K and 2 K warming relative to pre-industrial temperatures, respectively. The equilibrium response of glaciers to warming is non-linear, with a decreased sensitivity at higher temperatures, which is explained by the decreasing surface area and mass of glaciers available for melt.

Using an approximated linear relationship between global anthropogenic CO_2 emissions and global mean temperature change of 1700 Gt CO_2 emissions per 1 K of warming[26], we calculate the global glacier mass change commitment of

CO_2 emissions as a function of global mean temperature (Fig. 2). Since this mass change commitment is calculated from the equilibrium glacier mass, it is independent of, and additional to, any potential mass changes committed in the past, but not yet realized. We find that under present-day climate conditions, every emitted kg of CO_2 will eventually be responsible for a glacier mass loss of 14.8 (5.5 to 19.8) kg. Again, since the global glacier mass is decreasing with increasing temperatures, this number is greater for lower and smaller for higher temperatures.

These results indicate that a large fraction of glacier mass change projected for the 21st century[27, 28, 29, 30] will be a response to mass change commitments of the past. E.g., if global mean temperature was limited to rise to 1.5 K above pre-industrial values, as envisioned in the Paris Agreement, and kept at that value, about 70 % of the eventual glacier mass loss would be the realization of mass loss commitments originating from greenhouse gases emitted before the Paris Agreement. If the warming was limited to, and kept at, 2 K, this number would drop to about 60 %.

However, not all of the eventual mass change will be realized within the next century. We update projections of 21st century mass change[27] using a more recent glacier inventory (version 5, updated from version 1) and adding projections corresponding to 1.5 and 2.0 K of global mean temperature change above pre-industrial values. Since no CMIP5 projections dedicated to this goal exist so far, we scale temperature and precipitation anomaly fields from the RCP2.6 ensemble of CMIP5 to derive forcing fields for the glacier model (called 1.5 and 2 K scenarios from here on, see Methods for details). Timeseries of the resulting global mean temperature anomalies are shown in Fig. 3a. The differences between the RCP2.6 ensemble and 1.5 and 2 K scenarios are small. However, a significant difference between the RCP2.6 ensemble and the ensemble scaled to 1.5 K is detectable in the second half of the 20th century.

In all projections, glacier mass loss accelerates at least until the mid 21st century (Fig. 3b). No significant difference in global glacier mass change is detectable even between the RCP8.5 and the 1.5 k scenario until 2040. In the second half of the 21st century, for the low emission scenarios, glaciers strive towards a new equilibrium with climate conditions, expressed by lowering mass loss rates. In the high emission scenarios, mass loss accelerates well into the second half of the century. No significant difference can be detected between the 1.5 K and RCP2.6 scenarios, and only at the very end of the century between the 1.5 K and the 2 K scenarios.

From present day to the end of the 21st century, glaciers are projected to lose 76 (54 to 97) mm SLE under the 1.5 K scenario, 84 (54 to 116) mm SLE under the RCP2.6 scenarios, 89 (63-112) mm SLE under the 2 K scenario, 104 (58 to 136)mm SLE under the RCP4.5 scenario, 110 (75 to 140) mm SLE under the RCP6.0 scenario, and 142 (83-165) mm SLE under the RCP8.5 scenario (Fig. 3c). In global glacier mass, no significant difference is detectable within the 21st century between the 1.5, RCP2.6, and 2 K scenarios. A difference between the 1.5 K scenario and the RCP4.5 and RCP6.0 scenarios only emerges after 2080, and between the 1.5 K and the RCP8.5 scenarios after 2060.

Reductions of greenhouse gas emission will have a limited impact on 21st century glacier mass loss, as a large fraction of that mass loss and resulting run-off is the realization of past commitments. To a large degree, future glacier mass loss needs to be considered inevitable, making the identification and execution of appropriate adaptation measures mandatory. However, because of the nonlinear nature of global glacier mass sensitivity to global temperature change, more ambitious climate change mitigation measures will have a disproportionately greater impact on the long-term preservation of glaciers than less ambitious measures, reducing the required adaptive measures.

Figure 1: Global glacier equilibrium mass. Glacier mass is shown as change relative to present day (year 2015) mass as indicated by number, and as a function of global mean temperature change relative to pre-industrial (1850-1879). Small numbers indicate size of glacier model ensemble. Light (dark) shading indicates 5th to 95th (15th to 85th) percentile of the ensemble, black line is the ensemble median. Colored shading and lines on the right side indicate glacier equilibrium mass interpolated to different global mean temperatures, including present day (2006-2015) air temperature being 0.8 K above pre-industrial. Black ring indicates forcing with climate observations during the period 1961 to 1990. Upper horizontal axis (anthropogenic cumulative CO_2 emissions) is only approximated.

Figure 2: Global glacier mass change commitment as a function of global mean temperature change relative to pre-industrial (1850-1879). Light (dark) shading indicates 5th to 95th (15th to 85th) percentile of the glacier model ensemble, black line the ensemble median. Colored shading and line on the right side indicate values interpolated to present-day (2006-2015) temperature change.

Figure 3: Projections of global glacier mass change. a: global mean temperature anomalies relative to pre-industrial (1850-1879). b: glacier mass change rates. c: global glacier mass. Vertical lines indicate the 5th to 95th (thin) and 15th to 85th (thick) percentiles of the CMIP5 (panel a)/glacier model (panels b,c) ensembles at different times; time series show the ensemble median. Increased line thickness of time series indicates periods during which there is a significant difference to the ensemble scaled to Δ T = 1.5 K. Time series in panels a and b have been smoothed using a 10-year moving average for visual clarity.

References

[1] Gregory, J. M. *et al.* Twentieth-century global-mean sea-level rise: is the whole greater than the sum of the parts? *J. Climate* **26**, 4476–4499 (2013).

[2] Church, J. *et al.* Sea level change. In Stocker, T. *et al.* (eds.) *Climate Change 2013: The Physical Science Basis. Contribution of Working Group I to the Fifth Assessment Report of the Intergovernmental Panel on Climate Change* (Cambridge University Press, Cambridge, United Kingdom and New York, NY, USA, 2013).

[3] Richardson, S. D. & Reynolds, J. M. An overview of glacial hazards in the Himalayas. *Quaternary Int.* **65**, 31–47 (2000).

[4] Huggel, C., Clague, J. J. & Korup, O. Is climate change responsible for changing landslide activity in high mountains? *Earth Surface Processes and Landforms* **37**, 77–91 (2012).

[5] Jansson, P., Hock, R. & Schneider, T. The concept of glacier storage: a review. *J. Hydrol.* **282**, 116–129 (2003).

[6] Immerzeel, W. W., van Beek, L. P. H. & Bierkens, M. F. P. Climate change will affect the Asian water towers. *Science* **328**, 1382–1385 (2010).

[7] Huss, M. Present and future contribution of glacier storage change to runoff from macroscale drainage basins in Europe. *Water Resourc. Res.* **47**, W07511 (2011).

[8] Egholm, D., Nielsen, S., Pedersen, V. K. & Lesemann, J.-E. Glacial effects limiting mountain height. *Nature* **460**, 884–887 (2009).

[9] Thomson, S. N. *et al.* Glaciation as a destructive and constructive control on mountain building. *Nature* **467**, 313–317 (2010).

[10] Korup, O., Montgomery, D. R. & Hewitt, K. Glacier and landslide feedbacks to topographic relief in the himalayan syntaxes. *Proceedings of the National Academy of Sciences* **107**, 5317–5322 (2010).

[11] Oerlemans, J. Extracting a climate signal from 169 glacier records. *Science* **308**, 675–677 (2005).

[12] Kaser, G., Cogley, J. G., Dyurgerov, M. B., Meier, M. F. & Ohmura, A. Mass balance of glaciers and ice caps: Consensus estimates for 1961-2004. *Geophys. Res. Lett.* **33**, L19501 (2006). Doi:10.1029/2006GL027511.

[13] Marzeion, B., Jarosch, A. H. & Gregory, J. M. Feedbacks and mechanisms affecting the global sensitivity of glaciers to climate change. *The Cryosphere* **8**, 59–71 (2014).

[14] Jóhannesson, T., Raymond, C. & Waddington, E. Time-scale for adjustment of glaciers to changes in mass balance. *J. Glaciol.* **35**, 355–369 (1989).

[15] Bahr, D. B., Pfeffer, W. T., Sassolas, C. & Meier, M. F. Response time of glaciers as a function of size and mass balance: 1. theory. *Journal of Geophysical Research: Solid Earth* **103**, 9777–9782 (1998).

[16] Pelto, M. S. The current disequilibrium of North Cascade glaciers. *Hydrological Processes* **20**, 769–779 (2006).

[17] Huss, M. & Farinotti, D. Distributed ice thickness and volume of all glaciers around the globe. *J. Geophys. Res.* **117**, F04010 (2012).

[18] Grinsted, A. An estimate of global glacier volume. *The Cryosphere* **7**, 141–151 (2013).

[19] New, M., Lister, D., Hulme, M. & Makin, I. A high-resolution data set of surface climate over global land areas. *Clim. Res.* **21**, 1–25 (2002).

[20] Mitchell, T. D. & Jones, P. D. An improved method of constructing a database of monthly climate observations and associated high-resolution grids. *Int. J. Climatol.* **25**, 693–712 (2005).

[21] Pfeffer, W. T. *et al.* The Randolph Glacier Inventory: a globally complete inventory of glaciers. *J. Glaciol.* **60**, 537–552 (2014).

[22] Zemp, M. *et al.* Historically unprecedented global glacier decline in the early 21st century. *Journal of Glaciology* **61**, 745–762 (2015).

[23] Bahr, D. B., Dyurgerov, M. & Meier, M. F. Sea-level rise from glaciers and ice caps: A lower bound. *Geophys. Res. Lett.* **36**, L03501 (2009).

[24] Mernild, S. H., Lipscomb, W. H., Bahr, D. B., Radić, V. & Zemp, M. Global glacier retreat: a revised assessment of committed mass losses and sampling uncertainties. *The Cryosphere* **7**, 1565–1577 (2013).

[25] Marzeion, B., Cogley, J. G., Richter, K. & Parkes, D. Attribution of global glacier mass loss to anthropogenic and natural causes. *Science* **345**, 919–921 (2014).

[26] Stocker, T. *et al.* Technical summary. In Stocker, T. *et al.* (eds.) *Climate Change 2013: The Physical Science Basis. Contribution of Working Group I to the Fifth Assessment Report of the Intergovernmental Panel on Climate Change: Technical Summary* (Cambridge University Press, Cambridge, United Kingdom and New York, NY, USA, 2013).

[27] Marzeion, B., Jarosch, A. H. & Hofer, M. Past and future sea-level change from the surface mass balance of glaciers. *The Cryosphere* **6**, 1295–1322 (2012).

[28] Giesen, R. H. & Oerlemans, J. Climate-model induced differences in the 21st century global and regional glacier contributions to sea-level rise. *Climate Dyn.* **41**, 3283–3300 (2013).

[29] Bliss, A., Hock, R. & Radić, V. Global response of glacier runoff to twenty-first century climate change. *J. Geophys. Res.* **119**, 717–730 (2014).

[30] Huss, M. & Hock, R. A new model for global glacier change and sea-level rise. *Frontiers in Earth Science* **3**, 54 (2015).

Acknowledgments This work was funded by the German Federal Ministry of Education and Research (grant 01LS1602A), the German Research Foundation (grant MA 6966/1-1), and supported by the Austrian Ministry of Science BMWF as part of the UniInfrastrukturprogramm of the Research Platform Scientific Computing at the University of Innsbruck. We acknowledge the World Climate Research Programme's Working Group on Coupled Modelling, which is responsible for CMIP, and we thank the climate modeling groups (listed in the Table 1 of the supplementary material) for producing and making available their model output. For CMIP the U.S. Department of Energy's Program for Climate Model Diagnosis and Intercomparison provided coordinating support and led development of software infrastructure in partnership with the Global Organization for Earth System Science Portals. We thank Reto Stauffer and Axel Kreuter for their help with the figure design.

Competing Interests The authors declare that they have no competing financial interests.

Correspondence Correspondence and requests for materials should be addressed to B.M. (email: ben.marzeion@uni-bremen.de).

Author contributions BM, GK, and FM conceived the study and designed the experiments; BM performed the experiments and analyzed the results; BM and NC wrote the manuscript; all authors discussed the results and the manuscript.

Methods

Glacier model

The glacier model is set out in full in references [31, 27, 13, 25], on which the following description relies heavily. We refer the reader to these sources for further detail.

The glacier model is based on calculating the annual specific climatic mass balance B for each of the world's individual glaciers as

$$B = \left[\sum_{i=1}^{12} \left[P_i^{\text{solid}} - \mu^\star \cdot \max\left(T_i^{\text{terminus}} - T_{\text{melt}}, 0 \right) \right] \right] - \beta^\star \tag{1}$$

where P_i^{solid} is the monthly solid precipitation onto the glacier surface per unit area, which depends on the monthly mean total precipitation and the temperature range between the glacier's terminus and highest elevations (i.e., temperature at terminus elevation below a certain threshold implies all precipitation is solid, temperature at the glacier's maximum elevation above the threshold implies all precipitation is liquid, and within that temperature range, the precipitation fraction is interpolated linearly), $\mu^\star$ is the glacier's temperature sensitivity, T_i^{terminus} is the monthly mean air temperature at the glacier's terminus, T_{melt} is the monthly mean air temperature above which ice melt is assumed to occur, and $\beta^\star$ is a bias correction (see below). The model thus does not attempt to capture the full energy balance at the ice surface, but relies on air temperature as a proxy for the energy available for melt [32, 33, 34]. P_i^{solid} and T_i^{terminus} are determined based on gridded climate observations[19, 20], to which temperature and precipitation anomaly fields from the CMIP5 models are added (see Table 1 of the supplementary material). Changes affecting the glacier hypsometry (i.e. changes in its volume, surface area, and elevation range) are reflected in the determination of P_i^{solid} and T_i^{terminus}, which are modeled based on B, and on linearly adjusting the glacier's surface area and length towards their respective values obtained from volume-area and volume-length scaling [35, 36]. I.e., the surface area change $\mathrm{d}A$ of a glacier during each mass balance year t is calculated as

$$\mathrm{d}A(t) = \frac{1}{\tau_A(t)}\left(\left(\frac{V(t+1)}{c_A}\right)^{1/\gamma} - A(t)\right) \tag{2}$$

where $\tau_A(t)$ is the area relaxation time scale (see Eq. 5), $V(t+1)$ is the glacier's volume at the end of the mass balance year, $c_A = 0.0340$ km$^{3-2\gamma}$ (for glaciers), $c_A = 0.0538$ km$^{3-2\gamma}$ (for ice caps), $\gamma = 1.375$ (for glaciers), $\gamma = 1.25$ (for ice caps) are scaling parameters [35, 36], and $A(t)$ is the surface area of the glacier at the end of the preceding mass balance year. Similarly, length changes $\mathrm{d}L$ (and terminus elevation changes associated with them) during each mass balance year are estimated as

$$\mathrm{d}L(t) = \frac{1}{\tau_L(t)}\left(\left(\frac{V(t+1)}{c_L}\right)^{1/q} - L(t)\right) \tag{3}$$

where $\tau_L(t)$ is the length relaxation time scale (see Eq. 4), $c_L = 0.0180$ km^{3-q} (for glaciers), $c_L = 0.2252$ km^{3-q} (for ice caps), $q = 2.2$ (for glaciers), $q = 2.5$ (for ice caps) are scaling parameters [35, 36], and $L(t)$ is the glacier's length at the start of the mass balance year. The glacier length response time scale τ_L is estimated following roughly reference[14] as

$$\tau_L(t) = \frac{V(t)}{\sum_{i=1}^{12} \int P_{i,\text{clim}}^{\text{solid}}} \tag{4}$$

where $\int P_{i,\text{clim}}^{\text{solid}}$ is the monthly climatological solid precipitation integrated over the glacier surface area, calculated over the preceding 30 years. The glacier area response time scale is estimated as

$$\tau_A(t) = \tau_L(t)\frac{A(t)}{L(t)^2} \tag{5}$$

based on the assumption that area changes caused by glacier width changes occur instantaneously, while area changes caused by glacier length changes occur with the time scale of glacier length response.

The volume change dV of a glacier in year t is calculated as

$$dV(t) = B(t) \cdot A(t). \tag{6}$$

The temperature sensitivity $\mu^\star$ is determined from observed past variations for each of the glaciers with available mass balance observations [37, 38]. In these data sets, there are a global total of 255 glaciers that have all the metadata needed for the parameter estimation, that are covered by the temperature and precipitation data set we use (see below), that are indicated to be reliable, and that have at least two annual mass balance measurements. The procedure is as follows. We assume that there exists some 31-year reference period, centered on year $t^\star$, whose climatology is such that the glacier with its present-day hypsometry would be in equilibrium, i.e. with its mass not changing. For this reference period, by construction

$$B = \sum_{i=1}^{12}\left[P(t^\star)_{i,\text{clim}}^{\text{solid}} - \mu(t^\star)\cdot\left(\max\left(T(t^\star)_{i,\text{clim}}^{\text{terminus}} - T_{\text{melt}}, 0\right)\right)\right] = 0 \tag{7}$$

where $P(t^\star)_{i,\text{clim}}^{\text{solid}}$ and $T(t^\star)_{i,\text{clim}}^{\text{terminus}}$ are the monthly climatological values of P_i^{solid} and T_i^{terminus}, during the 31 year period centered around the year $t^\star$. Note that we do not assume $t^\star$ to be a time at which the glacier was actually in balance. If the climate has been warming and the glacier retreating, as is generally the case, $t^\star$ would be in the past, and the glacier actually would have had a negative mass balance at time $t^\star$. The assumption is that if the climate of time $t^\star$ had been maintained, the glacier eventually would have contracted until it reached its present-day hypsometry.

We obtain a total of 109 monthly climatologies of precipitation and temperature (the data set of reference[20] provides 109 years of monthly precipitation and temperature; at the end and beginning of the time series, the climatologies are calculated over shorter time periods), and subsequently obtain an estimate of μ from Eq. 7 for each of the 109 choices of $t^\star$. We then apply the glacier model to all glaciers for which direct mass balance observations are available, for each of the 109 possible values of $\mu(t)$. For each of these glaciers, we identify $t^\star$ as that time, for which applying the corresponding temperature sensitivity $\mu^\star \equiv \mu(t^\star)$ yields the smallest mean error of the modeled mass balances. This minimum difference is denoted by $\beta^\star$.

For glaciers without observed mass balances (i.e., the vast majority of glaciers), $t^\star$ is interpolated from the ten closest surrounding glaciers with mass balance observations, weighted inversely by distance. $\mu^\star$ is subsequently determined from solving Eq. 7 for $\mu^\star$, using precipitation and temperature obtained from the climatology centered around the interpolated value of $t^\star$. The bias correction $\beta^\star$ is determined by interpolating the minimized bias obtained during the determination of $t^\star$ from surrounding glaciers with mass balance observations.

$\mu^\star$ can vary greatly between neighbouring glaciers without obvious physical reasons, depending on glacier-specific issues such as avalanches, topographical shading, cloudiness, and other issues being related to systematic biases in the input data (e.g. climate, topography). By interpolating $t^\star$ instead of $\mu^\star$ for glaciers without mass balance observations, the constraint of $\mu(t)$ to not vary much with time is used, (i) to take into account the glacier-specific issues mentioned above (i.e., $\mu(t)$ will vary comparatively little around a given year t; errors in $t^\star$ – even large ones – will result in relatively small errors in $\mu^\star$), and (ii) to help compensate systematic biases in temperature and precipitation data. In that sense, the calibration procedure can be seen as an empirically driven downscaling strategy: if a glacier is located there, then the local climate (or the glacier temperature sensitivity) must allow a glacier to be there. For example, the effect of avalanches or a negative bias in precipitation input will have the same impact on calibration: the value of $\mu^\star$ will be lowered to take these effects into account, even though they are not resolved by the mass balance model. A cross validation of the determination of $\mu^\star$ shows that the spatial interpolation of $t^\star$ leads to substantially smaller errors than the spatial interpolation of $\mu^\star$ [27].

Initial values for surface area and elevation distribution of each glacier are obtained from the Randolph Glacier Inventory version 5. The model accounts for the differing dates of surface area measurement in the Randolph Glacier Inventory by ensuring that the observed glacier extent is reproduced in the year of observation.

Present day glacier mass is taken as a snapshot in the year 2015 from a transient reconstruction, with the model being forced by gridded climate observations[20]. Uncertainties (as given in Fig. 1) are based on the propagated model uncertainties obtained through the leave-one-glacier-out cross-validation described below. See references [27, 31] for details.

Validation of the glacier model and treatment of uncertainties

Uncertainty estimates of the glacier model are obtained by (i) performing a leave-one-glacier-out cross-validation that allows to determine the model's performance on glaciers without direct mass balance observations; (ii) propagating these uncertainties, and uncertainties of model parameters needed for, e.g., the estimation of the initial ice volume, through the entire glacier model, and (iii) validating these propagated and temporally accumulated uncertainties themselves, using independent geodetically measured volume and surface area changes[37].

The this second validation, the uncertainty estimates are found to be realistic. The systematic, global mean bias of the glacier model's annual specific glacier-wide mass balance is 5 mm water equivalent (not significantly different from zero).
Given any pair of glaciers for which the cross-validation is carried out, we may calculate the temporal correlation between the annual time series for those two glaciers of the errors in the modeled mass balance. Considering all such pairs, we can calculate the correlation of this temporal error correlation with the distance between the two glaciers. This latter correlation is < 0.01 (not significant), indicating that the model errors for the individual glaciers can be treated as independent of each other irrespective of their distance. The uncertainties for the globally aggregated data are thus obtained by taking the square root of the summed and squared uncertainties of the individual glaciers' results. A more detailed and complete description of the determination of the model's parameters, both glacier-specific and global, and of the comprehensive validation of the model, can be found in [27].
For scenario-based results, the total uncertainty is strongly dominated by ensemble spread, not glacier model uncertainty (e.g., for the RCP8.5 scenario, the uncertainty of the individual ensemble members is of the order of 5 mm SLE, the ensemble spread of the order of 100 mm SLE at the end of the 21st century). Uncertainties for these results are therefore given as the 5th to 95th percentile of the ensemble distribution.
For the equilibrium results, the uncertainties obtained through propagation and temporal accumulation in the glacier model are meaningless, since they are mostly a function of the model integration time. I.e., estimating the glaciers' equilibrium mass more accurately by integrating the glacier model for a longer time artificially inflates the propagated model uncertainty. Therefore, uncertainties are given as the 5th to 95th percentile of the ensemble distribution also in this case.
The uncertainty of the present day ice mass estimate (Figure 1) is obtained from the error propagation described above, applied to the glacier model forced by climate observations[20]. The ice mass estimate is slightly higher than an estimate obtained through a more elaborate method[39], but consistent with it considering the respective uncertainties.

Equilibrium experiments

Results from 15 different CMIP5 models, using the historical run continued by the RCP8.5 scenario (see Tab. 1 of the supplementary material), were used to force the glacier model in the equilibrium experiments over a range of global mean temperature anomalies. The RCP8.5 scenario was chosen in order to have the largest possible ensemble size also for relatively high global mean temperature anomalies.
For each of the combined historical and RCP8.5 experiments, monthly anomaly fields of precipitation and near surface air temperature were determined, relative to the monthly climatology of 1961 to 1990. Then, global mean temperature

anomalies were determined for each 30 year period contained in the combined historical and RCP8.5 experiment. From this data set, we obtained 30 year-long anomaly fields of precipitation and temperature, which correspond most closely to a given global mean temperature anomaly. Since the range of global mean temperature anomalies differs between the different CMIP5 models, also the number of anomaly fields extracted from each CMIP5 differs, leading to an ensemble size that depends on the global mean temperature anomaly considered (small numbers in Fig. 1). The anomaly fields were then added to the observed climatological fields of reference[19] to obtain the climate forcing for the glacier model. Additionally, the glacier model was forced by the observed climatological fields of reference[19] only, with temporal variability added from the same period from reference [20] (black cross in Fig. 1). Note that because of the temperature threshold sensitivity of the mass balance, also zero-mean temporal variability has a net effect on glacier volume, and identical mean temperatures can result in different glacier masses, as a result of different temporal variability. We express all temperature anomalies relative to the global mean temperature averaged between 1850 and 1879 in reference [40].

To obtain the equilibrium response of the glaciers to a given global mean temperature forcing, the same forcing (30 years) was repeatedly applied for each glacier until volume changes of the glacier became negligible. This was defined to be the case when the volume change over the last 100 modeled years was smaller than 1 % of the glacier volume. Reaching the equilibrium took up to approximately 700 years. On the global scale, ice volume changes are small after 200 years. Note that in an experimental setup like this, glaciers may reach an equilibrium, while the state of the climate system that was used to drive the glaciers into equilibrium is not itself a true equilibrium, but picked from a transient scenario.

To relate global mean temperature anomalies to anthropogenic CO_2 emissions (upper horizontal axis in Fig. 1, and calculations for Fig. 2), we assume a linear relation between the two based on Fig. TFE 8.1 in reference [26]. We estimate this relation to 1 K global mean temperature change per 1700 Gt CO_2 emissions.

Transient experiments

Transient experiments for the RCP2.6, RCP4.5, RCP6.0 and RCP8.5 scenarios were done exeactly as described in reference [27], except that the initial conditions for each glacier were updated to RGI version 5.0. To obtain a scenarios corresponding to 1.5 K and 2.0 K of warming, anomalies of CMIP5 RCP2.6 runs were scaled, using a time-dependent scaling factor: First, for each considered run, its global mean temperature anomaly during the period 2071 to 2100 was determined, as well as the associated scaling factor needed to bring it to 1.5 K or 2.0 K exactly. Then, starting in 2016 with a scaling factor of 1 (in order to avoid a discontinuity in the forcing fields), temperature anomaly fields were scaled down (or up), with the scaling factor increasing linearly in time until reaching it's pre-determined value at the end of the 21st century. This implies that for all scaled model runs, the global mean temperature during the last 30 years of the 21st century is exactly 1.5 K or 2.0 K above pre-industrial, which reduces the spread of the scaled model ensemble considerably. However, the temporal and spatial variability of each CMIP5 run are retained. It is unclear how precipitation anomalies should be related from the RCP2.6 scenario to the 1.5 K and 2.0 K scenarios. For the results shown here, we applied the same scaling factors used for the temperature anomaly fields also to the precipitation anomaly fields, based on the assumption that the amplitude of precipitation anomalies is linked to temperature anomalies [41]. While this relation should not be expected to hold regionally and at all times, it has very minor impacts on our results: to test the sensitivity of our results to this approach, we repeated the projections, leaving the precipitation anomaly fields unscaled. The differences to the results presented here were vanishingly small.

An alternative approach to scaling would be the selection of RCP2.6 ensemble members that end up close to 1.5 K or 2.0 K global mean temperature anomaly, as has been done in a regional study [42]. We prefer the scaling approach for two reasons: (i) it does not reduce the ensemble size, leading to more robust uncertainty statistics; (ii) it circumvents the possibility that selecting climate models that have a relatively low (or high) climate sensitivity leads to a reduction also in the spread of temporal and spatial climate variability.

To conclude whether the applied model chain is able to distinguish between the 1.5 K and the other scenarios, we perform a two-sample Kolmogorov-Smirnov test. For each year, we test at the $p < 0.05$ level against the null hypothesis that two ensembles, one of them being the 1.5 K scenario, are drawn from the same underlying population.

Data availability

The glacier model results and the scaled climate projections presented here are available from the corresponding author upon reasonable request.

References

[31] Marzeion, B., Leclercq, P., Cogley, J. & Jarosch, A. Brief communication: Global reconstructions of glacier mass change during the 20th century are consistent. *The Cryosphere* **9**, 2399–2404 (2015).

[32] Ohmura, A. Physical Basis for the Temperature-Based Melt-Index Method. *J. Appl. Meteorol.* **40**, 753–761 (2001).

[33] Hock, R. Temperature index melt modelling in mountain areas. *J. Hydrol.* **282**, 104–115 (2003).

[34] Sicart, J., Hock, R. & Six, D. Glacier melt, air temperature, and energy balance in different climates: The Bolivian Tropics, the French Alps, and northern Sweden. *J. Geophys. Res.* **113**, D24113 (2008).

[35] Bahr, D., Meier, M. & Peckham, S. The physical basis of glacier volume-area scaling. *J. Geophys. Res.* **102**, 355–362 (1997).

[36] Bahr, D. Global distributions of glacier properties: a stochastic scaling paradigm. *Water Resourc. Res.* **33**, 1669–1679 (1997).

[37] Cogley, J. G. Geodetic and direct mass-balance measurements: comparison and joint analysis. *Ann. Glaciol.* **50**, 96–100 (2009).

[38] WGMS (World Glacier Monitoring Service). Fluctuations of Glaciers 2005-2010 (2012).

[39] Huss, M. & Farinotti, D. Distributed ice thickness and volume of all glaciers around the globe. *J. Geophys. Res.* **117**, F04010 (2012).

[40] Morice, C. P., Kennedy, J. J., Rayner, N. A. & Jones, P. D. Quantifying uncertainties in global and regional temperature change using an ensemble of observational estimates: The HadCRUT4 data set. *J. Geophys. Res.* **117**, D08101 (2012).

[41] Andrews, T., Forster, P. M., Boucher, O., Bellouin, N. & Jones, A. Precipitation, radiative forcing and global temperature change. *Geophys. Res. Lett.* **37**, L14701 (2010).

[42] Kraaijenbrink, P., Bierkens, M., Lutz, A. & Immerzeel, W. Impact of a global temperature rise of 1.5 degrees celsius on Asia's glaciers. *Nature* **549**, 257–260 (2017).

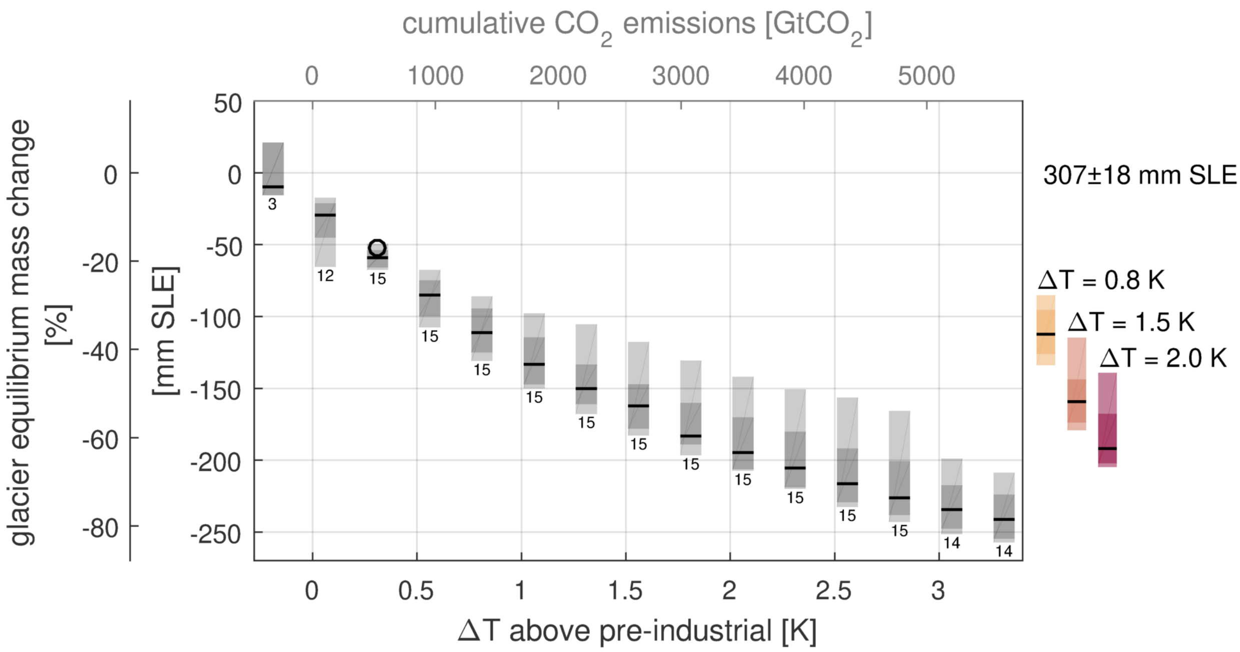

cumulative CO_2 emissions [$GtCO_2$]
0
1000
2000
3000
4000
5000
glacier equilibrium mass change [%]
0
-20
-40
-60
-80
[mm SLE]
50
0
-50
-100
-150
-200
-250
3
12
15
15
15
15
15
15
15
15
15
15
15
14
14
0
0.5
1
1.5
2
2.5
3
ΔT above pre-industrial [K]
307±18 mm SLE
ΔT = 0.8 K
ΔT = 1.5 K
ΔT = 2.0 K

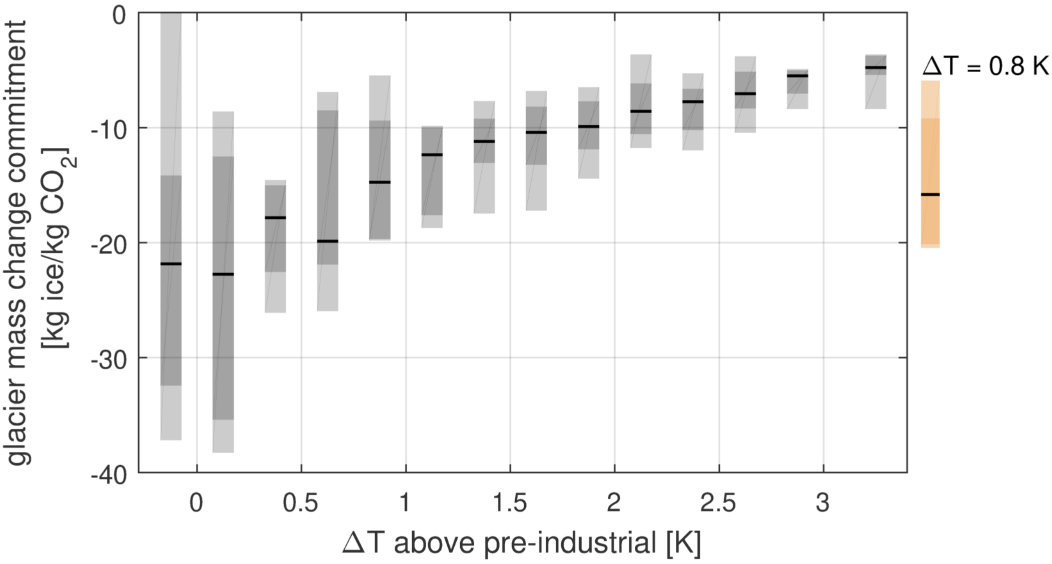

glacier mass change commitment
[kg ice/kg CO_2]
0
-10
-20
-30
-40
0
0.5
1
1.5
2
2.5
3
ΔT above pre-industrial [K]
ΔT = 0.8 K

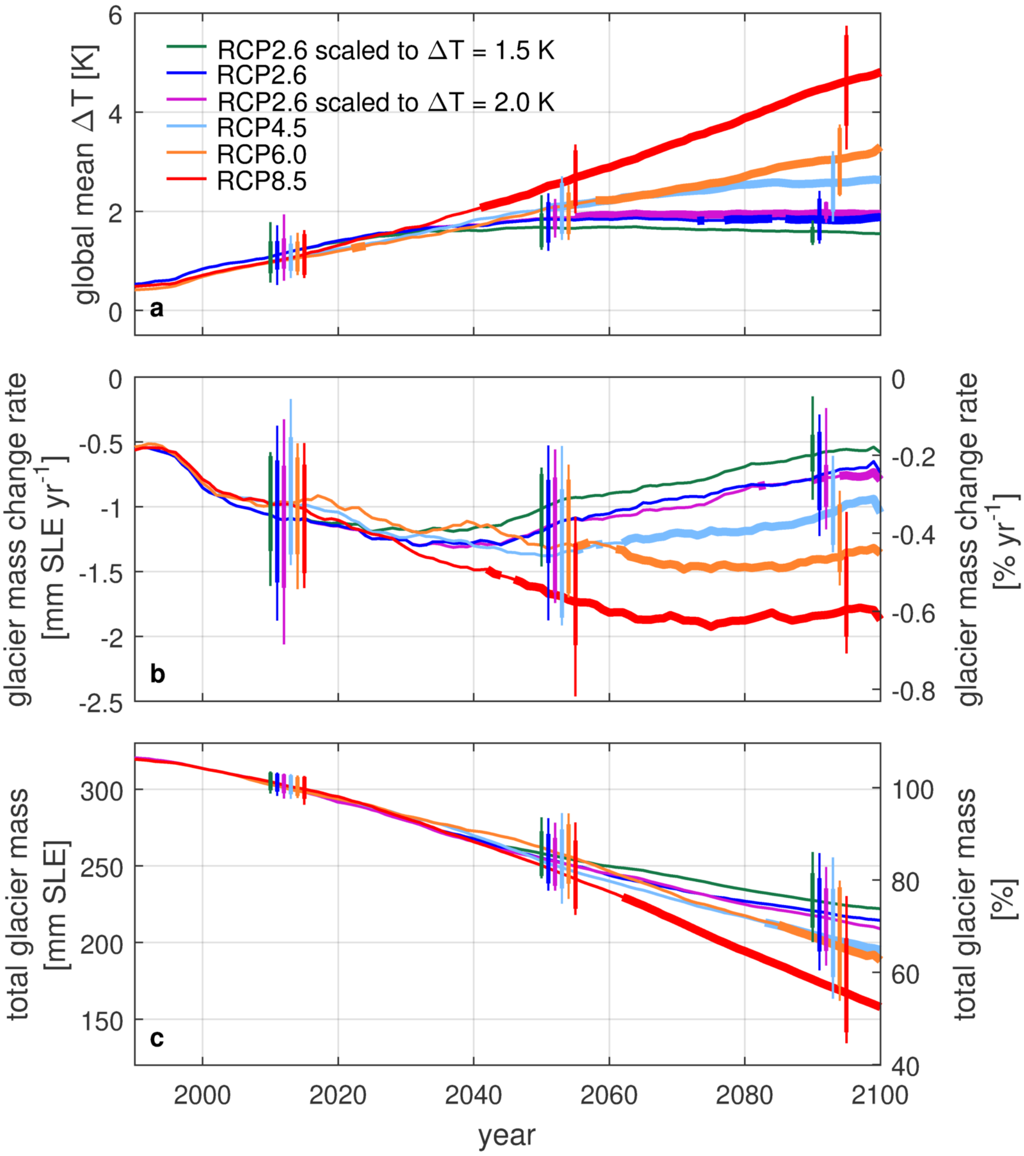

RCP2.6 scaled to ΔT = 1.5 K
RCP2.6
RCP2.6 scaled to ΔT = 2.0 K
RCP4.5
RCP6.0
RCP8.5
global mean ΔT [K]
a
glacier mass change rate [mm SLE yr-1]
glacier mass change rate [% yr-1]
b
total glacier mass [mm SLE]
total glacier mass [%]
c
year

Supplementary Material for the Manuscript *Limited influence of climate change mitigation on short-term glacier mass loss*

Ben Marzeion[1], Georg Kaser[2], Fabien Maussion[2] & Nicolas Champollion[1]

[1] *Institute of Geography, University of Bremen, Germany*

[2] *Department of Atmospheric and Cryospheric Sciences, Universität Innsbruck, Austria*

Table 1: Identifiers of CMIP5 model runs used in the study.

Model Name	historical	RCP2.6	RCP4.5	RCP6.0	RCP8.5
BCC-CSM1.1	r1i1p1	r1i1p1	r1i1p1	r1i1p1	r1i1p1
CanESM2	r1i1p1	r1i1p1	r1i1p1		r1i1p1
CCSM4	r1i1p1	r1i1p1	r1i1p1	r1i1p1	r1i1p1
CNRM-CM5	r1i1p1	r1i1p1	r1i1p1		r1i1p1
CSIRO-Mk3.6.0	r1i1p1	r1i1p1	r1i1p1	r1i1p1	r1i1p1
EC-EARTH	r1i1p1	r8i1p1			
FGOALS-s2	r1i1p1	r1i1p1			
GFDL-CM3	r1i1p1	r1i1p1	r1i1p1	r1i1p1	r1i1p1
GISS-E2-R	r1i1p1		r1i1p1	r1i1p1	r1i1p1
HadGEM2-ES	r1i1p1	r1i1p1	r1i1p1	r1i1p1	r1i1p1
inmcm4	r1i1p1		r1i1p1		r1i1p1
IPSL-CM5A-LR	r1i1p1	r1i1p1	r1i1p1	r1i1p1	r1i1p1
MIROC5	r1i1p1	r1i1p1	r1i1p1	r1i1p1	r1i1p1
MIROC-ESM	r1i1p1	r1i1p1	r1i1p1	r1i1p1	r1i1p1
MPI-ESM-LR	r1i1p1	r1i1p1	r1i1p1		r1i1p1
MRI-CGCM3	r1i1p1	r1i1p1	r1i1p1	r1i1p1	r1i1p1
NorESM1-M	r1i1p1	r1i1p1	r1i1p1	r1i1p1	r1i1p1
ensemble size	17	15	15	11	15